Band-gap corrected density functional theory calculations for InAs/GaSb type II superlattices

Jianwei Wang and Yong Zhang

Citation: Journal of Applied Physics **116**, 214301 (2014); doi: 10.1063/1.4903063
View online: http://dx.doi.org/10.1063/1.4903063
View Table of Contents: http://scitation.aip.org/content/aip/journal/jap/116/21?ver=pdfcov
Published by the AIP Publishing

Band-gap corrected density functional theory calculations for InAs/GaSb type II superlattices

Jianwei Wang and Yong Zhang
Department of Electrical and Computer Engineering, The University of North Carolina at Charlotte, 9201 University City Boulevard, Charlotte, North Carolina 28223, USA

(Received 24 September 2014; accepted 19 November 2014; published online 1 December 2014)

We performed pseudopotential based density functional theory (DFT) calculations for GaSb/InAs type II superlattices (T2SLs), with bandgap errors from the local density approximation mitigated by applying an empirical method to correct the bulk bandgaps. Specifically, this work (1) compared the calculated bandgaps with experimental data and non-self-consistent atomistic methods; (2) calculated the T2SL band structures with varying structural parameters; (3) investigated the interfacial effects associated with the no-common-atom heterostructure; and (4) studied the strain effect due to lattice mismatch between the two components. This work demonstrates the feasibility of applying the DFT method to more exotic heterostructures and defect problems related to this material system. © *2014 AIP Publishing LLC*.
[http://dx.doi.org/10.1063/1.4903063]

I. INTRODUCTION

The electronic structures of GaSb/InAs type II superlattices (T2SLs) were first studied theoretically in the1970s.[1,2] Since then, a number of theoretical studies have been performed on various aspects of the T2SL—most were related to its applications in IR detection.[3–16] This material system has been shown to be one of the most promising alternatives to the more technically developed HgCdTe, especially for mid- and long-wave IR detection.[17] More recently, GaSb/InAs double-heterostructures have been proposed and explored for other fundamental interests in physics, such as Bose-Einstein condensation of excitons[18] and the quantum spin Hall effect.[19]

An intriguing and important aspect of GaSb/InAs lies in its extreme type-II energy alignment, namely, the conduction band minimum (CBM) of InAs is lower than the valence band maximum (VBM) of GaSb. In principle, this allows one to achieve any desirable long wave IR bandgap for IR detection, and even a negative bandgap for more exotic physics by adjusting the superlattice layer widths. The electronic structures of the GaSb/InAs T2SL or heterostructure have mostly been calculated in the framework of k·p theory that has been widely used for many semiconductor superlattices.[3,5,7,9,10,16,19] A few exceptions exist using atomistic theories: the linear combination of atomic orbitals (LCAO) method,[2] empirical tight binding method (ETBM),[6,11] empirical pseudopotential method (EPM),[12–14] and the atomic orbital potential method with a general gradient approximation (GGA).[15]

The empirical methods have been rather successful in predicting SL band gaps and aiding in device design. The k·p method uses an effective-mass approximation, which makes it insufficient for describing the electronic structure of a very thin superlattice. Another more important issue is that of the non-trivial interface effect in a superlattice with no-common atom such as GaSb/InAs, which is not accounted for in the conventional k·p based theory, although some additional terms could be empirically introduced to mitigate the symmetry breaking effects due to the interfaces.[20,21] The non-self-consistent atomistic methods, for instance EPM,[13,14] can indeed naturally take into account the interfacial and symmetry breaking effects. However, non-self-consistent methods cannot properly treat more subtle effects, such as charge transfer near the interface, which is expected to be more significant for very thin layers. The attempted use of a self-consistent method[16] encountered the well-known local density approximation (LDA) bandgap error problem, which is more prominent in a type II heterostructure. The widely applied "scissor" correction to the bandgap was found inadequate for generating an accurate bandgap because the bandgap errors were not the same for the two heterostructure components. The density functional theory (DFT), as a self-consistent method, has been a powerful tool for studying the electronic properties of materials. However, it has rarely been used for T2SLs, largely due to the bandgap error with either LDA or GGA, which often results in a negative bandgap instead of a small positive bandgap.

II. BAND-GAP CORRECTION AND COMPUTATIONAL DETAILS

In this work, we implemented an atomistic bandgap correction scheme to correct the LDA band gap error, and therefore were able to predict the electronic structure of the T2SL using the first-principles method, and applied it to further study interfacial effects. The primary aim of this work is to study the electronic structure of the T2SL for IR detection. The method can be applied for other heterostructures as mentioned above. Furthermore, this work establishes a framework for investigating defects in the T2SL using DFT, which was in fact our ultimate goal when initiating this work, and is pertinent for improving the performance of the T2SL IR detector. Our approach can provide the similar or even improved results for GaSb/InAs T2SLs bandgaps when compared with the EPM results and experimental data. Additionally, the strain in the T2SL was calculated and

compared with a recently available experimental result that demonstrated strong interlayer diffusion.[22]

A plane-wave pseudopotential code, PEtot,[23] was used for self-consistent calculations. The d electrons were included in the norm-conserving pseudopotentials of Ga and In atoms, with a kinetic energy cutoff of 60 Ry. A Monkhorst–Pack k-point mesh of $6 \times 6 \times 1$ was used. Spin-orbit coupling was included using the PESCAN code.[24] The superlattice structure was fully relaxed in the LDA with the in-plane (x-y) lattice constant kept at the calculated bulk GaSb value of 6.043 Å (experimental value of 6.087 Å), in order to simulate the growth using GaSb substrate. Whereas the atomic positions and the out-of-plane (z) lattice constant were allowed to vary until the total energy was minimized. The correction to the LDA error was done by introducing empirical corrections to s, p, and d components of atomic pseudopotentials[25] after the self-consistent calculation. The pseudopotential corrections were obtained by adjusting the bulk DFT electronic structures of GaSb and InAs to their experimental values or quasiparticle calculation results when reliable experimental values were not available. This approach has been used successfully in predicting the impurity energy levels and alloy band gaps, typically with an accuracy within a few meV, in various semiconductor systems, such as GaAs:N,[25] GaP:N,[26] GaInP alloy,[27] and GaAs:Bi.[28] For bulk materials in their experimental lattice constants, the band gaps at Γ, X, and L points after (before) applying the corrections for GaSb and InAs are $E_{g\Gamma} = 0.810\,(-0.168)$ eV, $E_{\mathbf{gX}} = 1.248\,(0.650)$ eV, $E_{\mathbf{gL}} = 0.931\,(0.167)$ eV; and $E_{g\Gamma} = 0.422\,(-0.318)$ eV, $E_{\mathbf{gX}} = 1.986\,(1.454)$ eV, $E_{\mathbf{gL}} = 1.635\,(0.845)$ eV, respectively.

III. ELECTRONIC STRUCTURES

First, to test the accuracy of our approach for calculating the superlattice band structures, we investigated $(GaSb)_N/(InAs)_8$ with N = 8 to 40, where N is the number of monolayers, and compared these results with experimental data[29,30] and previous EPM results.[14] A graph comparing the lowest gaps is shown in Fig. 1; higher subband transition energies are tabulated in Table I. Apparently, for the fundamental bandgap, our values are closer to the experimental data than the EPM results. Furthermore, our values are slightly higher than the experimental results, which is in fact expected based on two considerations: (1) the inter-layer atomic diffusion tends to lower the bandgap from that predicted assuming abrupt interfaces. A recent X-ray diffraction study has indeed revealed substantial atomic intermixing between layers even in a best available GaSb/InAs T2SL grown by MBE.[22] The impact on the band structure is less severe for the lowest bandgap but likely more significant for higher bandgaps, which may explain the larger deviations in our calculated higher subband energies compared to the experimental data, as shown in Table I. (2) The exciton binding energy has not been included in the calculation, which may also contribute to the deviation, but perhaps to a lower extent. In contrast, the EPM results were already lower than the experimental results before accounting for the above mentioned effects. This comparison indicates that our DFT based approach is capable of predicting a superlattice bandgap with very good accuracy.

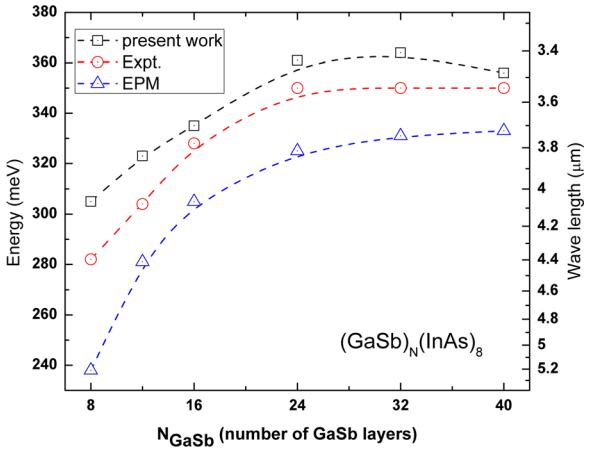

FIG. 1. Calculated transition energies from the first valence subband to the first conduction band. The black squares indicate our calculated results, the red circle the experimental values,[29,30] and the blue triangle the results calculated by EPM.[14]

Second, we applied this approach to investigate the effects of varying GaSb and InAs layer thickness, respectively, while keeping one component thickness fixed. Specifically, $(GaSb)_N(InAs)_{10}$ and $(GaSb)_{10}(InAs)_N$ with N = 2–10 were considered. The calculated band gaps for these structures are plotted in Fig. 2(a), and the respective CBM and VBM energy levels appear in Fig. 2(b) with respect to the bulk GaSb VBM. As shown in Fig. 2(a), starting from N = 10 and reducing the monolayer number N leads to an increase in bandgap, which is more effective by changing the InAs rather than GaSb layer thicknesses. The contrast variation in the two cases is because of that for the former case the electron confinement energy of the InAs layer thickness is changed, whereas for the latter case the hole confinement energy of the GaSb layer is varied, and the electron effective mass is much lower than the hole effective mass. The shifts of the band edges in Fig. 2(b) reflect the changes in band alignment with varying a layer thickness. The trends can be qualitatively understood in terms of the change in quantum confinement for the electron and hole.

TABLE I. Calculated transition energies (unit: meV) from the different valence subbands to the lowest conduction band CB1. The experimental values[29,30] are indicated by round bracket and the empirical pseudopotential results in square brackets. (Reference 14 and references therein).

InAs/GaSb	CB1-VB1	CB1-VB2	CB1-VB3	CB1-VB4
8/8	305	460	518	
	(282)[238]	(402)[378]	(670)[494]	
8/12	323	417	456	
	(304)[281]	(381)[383]	(516)[428]	
8/16	335	398	423	
	(328)[305]	(370)[378]	(464)[406]	
8/24	361	397	408	453
	(350)[325]	(364)[364]	(397)[387]	(487)[445]
8/32	364	385	390	421
	(350)[331]	(363)[355]	(381)[373]	(433)[404]
8/40	354	399	418	442
	(350)[333]	(362)[348]	(376)[363]	(409)[381]

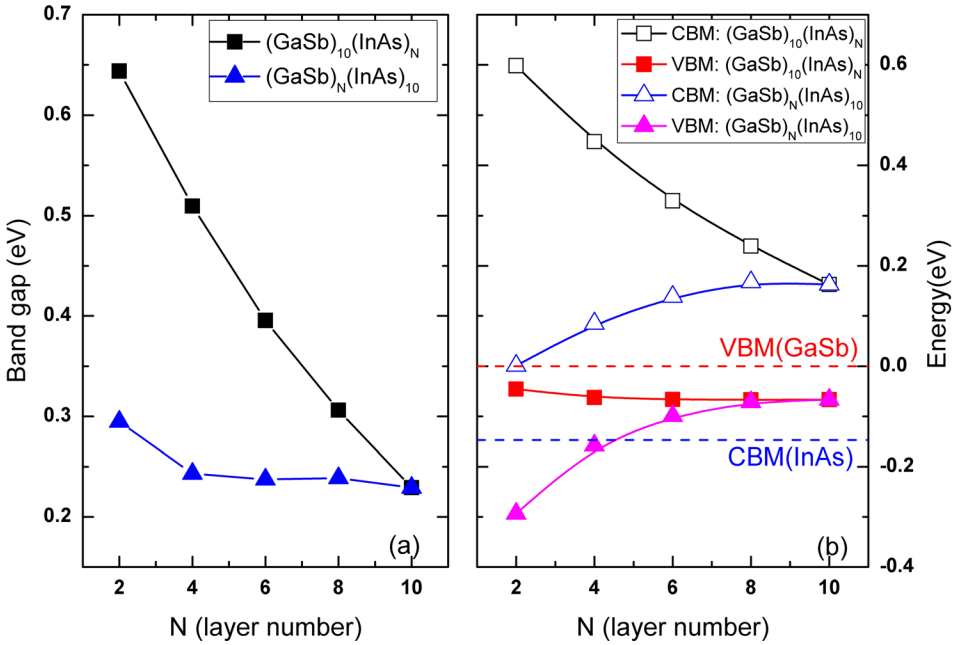

FIG. 2. The electronic structures of $(GaSb)_{10}(InAs)_N$ and $(GaSb)_N(InAs)_{10}$ [001] superlattices with varying monolayer number N: (a) band gaps and (b) band edge energies.

Our calculated band gap for $(GaSb)_{10}(InAs)_{10}$ is 229 meV, which is very close to the available experimental results: ~240 meV,[13] 230 meV,[31,32] and ~220 meV.[33] The band gap of a similar structure, $(GaSb)_{10}/(InSb)_1/(InAs)_{10}$, was predicted to be 216.8 meV by a k·p method[9] and 170.7 meV by the empirical "scissor" corrected self-consistent calculation.[15] These comparisons again confirm the high accuracy of our approach.

When keeping $N_{GaSb} = 10$ and changing N_{InAs} from 2 to 10, we found that the bandgap decreases from 644 meV to 229 meV or a 415 meV reduction. This decrease in bandgap is primarily due to the lowering of CB1 by 388 meV. Our finding is qualitatively consistent to that of a previous ETBM calculation[6] with a sp^3s^* basis. However, when N_{InAs} is kept at a constant of 10 while N_{GaSb} is increased from 2 to 10, the reduced magnitudes in CB1 and VB1 are comparable, and their differences lead to smaller band gap changes, an overall 66 meV changes. The sensitivity of the CBM to the InAs layer thickness is important for achieving a semiconductor-to-semimetal phase transition and studying related quantum spin Hall and topological insulating effects, although in this study, our focus is on structures that behave like a direct bandgap semiconductor intended for IR detection.

Third, we examined the unique interfacial effects associated with the no-common-atom superlattice like GaSb/InAs as opposed to with-common-atom superlattices like GaAs/AlAs. There are three possible interfacial arrangements that can, in principle, be realized and controlled by adjusting the growth conditions, assuming that the interfaces are idealistic (i.e., no interlayer mixing). We used the $(GaSb)_8/(InAs)_8$ structure to illustrate the variations. Its formula $(GaSb)_8/(InAs)_8$ implicitly implies the co-existence of one interfacial monolayer of GaAs and one interfacial monolayer of InSb at the interfaces of one superlattice period, which is commonly referred to as a "neutral" structure. One variation is to remove the GaAs monolayer by growing $(GaSb)_8/(InSb)_1/(InAs)_7$, which is referred to as a "heavy" interface structure. The other variation is to remove the InSb monolayer by growing $(GaSb)_7/(GaAs)_1/(InAs)_8$, which is referred to as a "light" interface structure. The bandgaps of three structures are found to vary slightly: 305 meV ("neutral"), 292 meV ("heavy"), and 358 meV ("light"). However, there are some interesting changes in the wave-functions of the different sub-bands, as shown in Fig. 3 for the in-plane averaged wave-function square along the [001] direction for a few important band edge states: the first and second valence sub-bands (VB1 and VB2), the first conduction sub-band (CB1), and the interfacial state localized at the GaAs interfacial layer (CB_{GaAs}). As expected, CB1 tends to localize in the InAs layer but with some leakage into the GaSb layer. VB1 is mostly localized in the GaSb layer, which explains the two well-known limitations of the T2SL: (1) the absorption strength near the fundamental band edge, corresponding to VB1–CB1 transition, is expected to be much weaker (as shown experimentally[31]) than that in a direct bandgap bulk material or type I superlattice, and (2) the vertical transport, for the hole state in particular, is limited.[16] An alternative device geometry based on a core-shell nanowire array could, in principle, alleviate these two shortcomings by increasing the interface area, improving carrier separations, and changing transport direction.[34]

The interfaces effects on the band edge states can be summarized as follows: CB1 avoids the InSb interface and prefers the GaAs interface, whereas the opposite is true for VB1, as shown for the "neutral" structure. Therefore, CB1 experiences greater confinement to the center of the InAs region with two InSb interfaces (the "heavy" structure), and is less confined with two GaAs interfaces (the "light" structure). In contrast, VB1 demonstrated greater confinement to the GaSb region with two GaAs interfaces present, and was more spread out with two InSb interfaces. These findings are qualitatively similar to those of the EPM study.[14] For VB1, the computational results can be qualitatively understood by considering the relative band

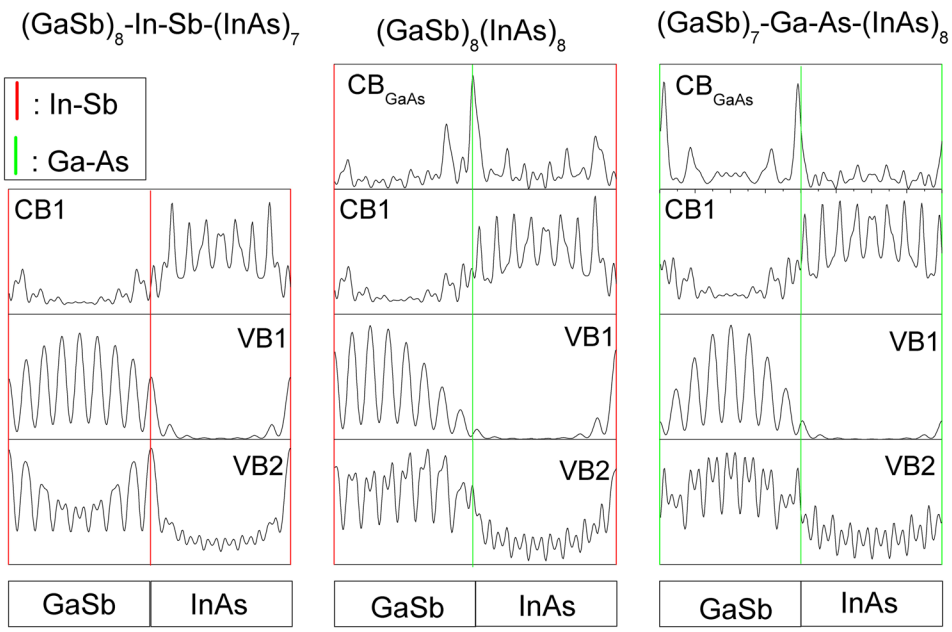

FIG. 3. In-plane averaged squares of wave functions at the Brillouin zone center for selected energy levels for three different interfacial structures: $(GaSb)_8$-In-Sb-$(InAs)_7$, $(GaSb)_8(InAs)_8$, and $(GaSb)_7$-Ga-As-$(InAs)_8$. The red line indicates the In-Sb interface and the green line the Ga-As interface.

alignments among the related materials: the InSb (GaAs) VBM is higher (lower) than for GaSb. However, CB1 is counterintuitive, since the CBMs for both GaAs and GaSb are substantially higher than for InAs,[35] although the in-plane tensile strain might significantly lower the GaAs state. We have further identified a resonant conduction band state (at 0.640 eV in $(GaSb)_8(InAs)_8$ and 0.698 eV in $(GaSb)_7$-Ga-As-$(InAs)_8$ above their respective CB1) that is strongly localized at the GaAs interface(s), hereafter referred to as the GaAs interface state, which does not exist in the $(Ga\text{-}Sb)_8$-In-Sb-$(InAs)_7$ structure.

IV. STRAIN EFFECT

We examined the strain effects due to the lattice mismatch between GaSb and InAs when grown on GaSb substrate using the parameters of a real sample (21 Å GaSb)/(44 Å InAs) obtained from readily available experimental data.[10,22] The in-plane lattice parameter is assumed to be the optimized bulk GaSb lattice constant of 6.043 Å (0.7% lower than the experimental value of 6.0875 Å). The optimized bulk lattice parameter of InAs is 6.020 Å (0.6% lower than the experimental value of 6.0583 Å). The InAs layers are assumed to be coherently strained to the GaSb substrate. The structure is simulated by a $(GaSb)_7/(InAs)_{15}$ supercell, which is closest structurally to a real sample. The structure has an optimized period of 66.0 Å along the superlattice axis compared to the unrelaxed period of 66.30 Å. The averaged lattice constant along the superlattice axis is predicted to be 0.7% smaller than that of GaSb substrate, whereas the experimental result was found to be −0.26%.[22] This discrepancy is most likely due to the fact that the calculation assumes abrupt interfaces but the real structure has been shown to exhibit rather strong inter-layer diffusion.[22] Nevertheless, the calculated bandgap of 0.142 eV is reasonably close to the estimated value of 0.130 eV obtained from a PL measurement.[10]

V. CONCLUSIONS

We have applied a band-gap corrected DFT-LDA approach to investigate the electronic structure and strain effects in GaSb/InAs T2SLs. This method can yield more accurate superlattice bandgaps by varying the structural parameters, compared with experimental data than non-self-consistent atomistic methods. The interfacial effects associated with the no-common-atom superlattice structure are studied. The conduction band edge is found to avoid the InSb interface and to prefer the GaAs interface, whereas the opposite is true for the valence band edge. An interface state localized at the GaAs interface is found to be in resonance with the conduction band. The lattice strain is calculated assuming abrupt interfaces, and comparison with the experimental data indicates that it is necessary to account for the interlayer atomic diffusion. Although the interlayer diffusion may not strongly affect the lowest bandgap, it could have a significant effect for high subbands. These calculated bandgaps show larger deviations from the experimental data.

ACKNOWLEDGMENTS

We thank supports from U.S. ARO/MURI Program (Grant No. Army W911NF-10-1-0524 and monitored by Dr. William Clark) and Bissell Distinguished Professorship, and Dr. Lin-Wang Wang for providing the computational codes and helpful discussions.

[1]G. A. Sai-Halasz, R. Tsu, and L. Esaki, Appl. Phys. Lett. **30**, 651 (1977).
[2]G. A. Sai-Halasz, L. Esaki, and W. A. Harrison, Phys. Rev. B **18**, 2812 (1978).
[3]D. L. Smith and C. Mailhiot, J. Appl. Phys. **62**, 2545 (1987).
[4]D. Z. Y. Ting, E. T. Yu, D. A. Collins, D. H. Chow, and T. C. McGill, J. Vac. Sci. Technol., B **8**, 810 (1990).
[5]C. H. Grein, P. M. Young, and H. Ehrenreich, Appl. Phys. Lett. **61**, 2905 (1992).
[6]J. Shen, S. Y. Ren, and J. D. Dow, Phys. Rev. B **46**, 6938 (1992).
[7]C. H. Grein, P. M. Young, and H. Ehrenreich, J. Appl. Phys. **76**, 1940 (1994).
[8]G. J. Brown, S. Houston, and F. Szmulowicz, Physica E **20**, 471 (2004).

[9]X.-L. Lang and J.-B. Xia, J. Appl. Phys. **113**, 043715 (2013).
[10]P.-F. Qiao, S. Mou, and S. L. Chuang, Opt. Express **20**, 2319 (2012).
[11]Y. Wei and M. Razeghi, Phys. Rev. B **69**, 085316 (2004).
[12]L. W. Wang, S. H. Wei, T. Mattila, A. Zunger, I. Vurgaftman, and J. R. Meyer, Phys. Rev. B **60**, 5590 (1999).
[13]G. C. Dente and M. L. Tilton, Phys. Rev. B **66**, 165307 (2002).
[14]R. Magri and A. Zunger, Phys. Rev. B **65**, 165302 (2002).
[15]W.-F. Sun, M.-C. Li, and L.-C. Zhao, Superlattices Microstruct. **49**, 81 (2011).
[16]F. Szmulowicz, H. J. Haugan, S. Elhamri, and G. J. Brown, Phys. Rev. B **84**, 155307 (2011).
[17]E. A. Plis, Adv. Electron. **2014**, 246769 (2014).
[18]Y. Naveh and B. Laikhtman, Phys. Rev. Lett. **77**, 900 (1996).
[19]C. Liu, T. L. Hughes, X.-L. Qi, K. Wang, and S.-C. Zhang, Phys. Rev. Lett. **100**, 236601 (2008).
[20]E. L. Ivchenko, A. Y. Kaminski, and U. Rössler, Phys. Rev. B **54**, 5852 (1996).
[21]F. Szmulowicz, H. Haugan, and G. J. Brown, Phys. Rev. B **69**, 155321 (2004).
[22]Y. Meng, H. Kim, J.-L. Rouviére, D. Isheim, D. N. Seidman, and J.-M. Zuo, J. Appl. Phys. **116**, 013513 (2014).
[23]See http://cmsn.lbl.gov/html/PEtot/PEtot.html for information about PEtot code.
[24]See http://cmsn.lbl.gov/html/Escan/DOE-nano/pescan.htm for information about PESCAN code.
[25]L.-W. Wang, Appl. Phys. Lett. **78**, 1565 (2001).
[26]Y. Zhang, A. Mascarenhas, and L. W. Wang, Phys. Rev. B **74**, 041201 (2006).
[27]Y. Zhang, A. Mascarenhas, and L.-W. Wang, Phys. Rev. B **63**, 201312 (2001).
[28]Y. Zhang, A. Mascarenhas, and L. W. Wang, Phys. Rev. B **71**, 155201 (2005).
[29]R. Kaspi, C. Moeller, A. Ongstad, M. L. Tilton, D. Gianardi, G. Dente, and P. Gopaladasu, Appl. Phys. Lett. **76**, 409 (2000).
[30]A. P. Ongstad, R. Kaspi, C. E. Moeller, M. L. Tilton, D. M. Gianardi, J. R. Chavez, and G. C. Dente, J. Appl. Phys. **89**, 2185 (2001).
[31]J. B. Rodriguez, P. Christol, L. Cerutti, F. Chevrier, and A. Joullié, J. Cryst. Growth **274**, 6 (2005).
[32]P. Christol, L. Konczewicz, Y. Cuminal, H. Aït-Kaci, J. B. Rodriguez, and A. Joullié, Phys. Status Solidi C **4**, 1494 (2007).
[33]B. Satpati, J. B. Rodriguez, A. Trampert, E. Tournié, A. Joullié, and P. Christol, J. Cryst. Growth **301–302**, 889 (2007).
[34]Y. Zhang, L.-W. Wang, and A. Mascarenhas, Nano Lett. **7**, 1264 (2007).
[35]Y. Zhang and W. Ge, J. Lumin. **85**, 247 (2000).